Available online at www.sciencedirect.com
ScienceDirect
Journal of Sound and Vibration 323 (2009) 426–443
JOURNAL OF SOUND AND VIBRATION
www.elsevier.com/locate/jsvi

Accurate in-plane free vibration analysis of rectangular orthotropic plates

D.J. Gorman

Department of Mechanical Engineering, The University of Ottawa, 770 King Edward Avenue, Ottawa, Canada K1N 6N5

Received 10 June 2008; received in revised form 17 December 2008; accepted 17 December 2008
Handling Editor: S. Bolton
Available online 7 February 2009

Abstract

Accurate analytical type solutions are obtained for the free in-plane vibration eigenvalues and mode shapes of fully clamped orthotropic rectangular plates. Appropriate governing differential equations for orthotropic plates are developed in dimensionless form and employed. Solutions are obtained by the method of superposition. It will be apparent that the solution procedure can be readily extended to analyze plates with other types of classical boundary conditions. The work reported is a natural extension of earlier work related to the in-plane vibration of isotropic plates. This appears to be the first analytical type study related to orthotropic plate in-plane vibration. It is expected that results tabulated here will form a valuable reference against which the results of other researchers may be compared.

1. Introduction

It is generally agreed that the amount of research devoted to free in-plane vibration of rectangular plates is extremely small in comparison to that devoted to free transverse vibration of the same plates. A listing of some of the more recent publications dealing with in-plane vibration is provided by Bardell et al. [1]. Designers of elastic structures have traditionally been more interested in the plate transverse vibration which can be excited by forces of relatively low frequencies. Nevertheless, it remains a fact that excitation of in-plane vibration, with higher associated natural frequencies, can occur when thin plates are subjected to high speed tangential flows, for example.

In recent years the present author has been involved in furthering research related to in-plane rectangular plate free vibration. He has introduced the superposition method for resolving these problems (see for example Refs. [2–4]). This method has already been employed very successfully in the analysis of rectangular plate transverse vibration. Excellent agreement has been obtained when computed results were compared with the findings of Bardell et al. [1]. A more recent paper dealing with elastically restrained edges has been published by Du et al. [5]. They describe a mathematical approach for analysis of in-plane vibration of rectangular isotropic plates supported by general elastic boundary conditions. They refer to this as "an analytical method" although it is the present writer's understanding that any method which expresses the displacement solutions as a summation of continuous differentiable functions constitutes an analytical method. This would include the superposition method or the Ritz method, for example, but not the finite element method.

E-mail address: dgorman@genie.uottawa.ca

0022-460X/$ - see front matter © 2009 Elsevier Ltd. All rights reserved.
doi:10.1016/j.jsv.2008.12.021

Nomenclature

a,b	dimensions of quarter plate
E_x, E_y	Youngs moduli related to the x and y directions, respectively
E_y/E_x	stiffness ratio
Eta	symbol used for coordinate η of Figs. 7–12
G_{xy}	modulus of elasticity in shear
K	number of terms used in building block solutions
Psi	symbol used for coordinate ξ in Figs. 7–12
t	time
u,v	displacements in x and y directions, respectively
U,V	dimensionless displacements u/a and v/b, respectively
x,y	plate rectangular coordinates
σ_x,σ_y	normal stresses related to x and y directions, respectively
$\sigma_x{}^*,\sigma_y{}^*$	dimensionless normal stresses, defined in text
τ_{xy}	shear stress
$\tau_{xy}{}^*$	dimensionless shear stress defined in text
ξ,η	dimensionless coordinates x/a and y/b, respectively
ρ	mass density of plate material
ν_x,ν_y	Poisson ratios related to x and y directions, respectively
$\varepsilon_x,\varepsilon_y$	longitudinal strain in x and y directions, respectively
ϕ	plate aspect ratio, b/a
λ^2	dimensionless frequency, $=\omega a\sqrt{\rho(1-\nu_x\nu_y)/E_x}$

They take their displacement solutions in the form of double Fourier series augmented by single Fourier series, the latter series being pre-multiplied by selected polynomials. The solutions thus formulated are constrained to satisfy the prescribed boundary conditions. This requires obtaining Fourier expansions for the polynomials referred to above. Finally, the constrained forms of the displacement expansions are substituted into the governing differential equations in order to develop a truncated matrix from which the problem eigenvalues are extracted.

In the abstract the authors state that the in-plane displacements are expressed through the superposition of two Fourier type expansions. In this writer's view what is employed is a summation of series solutions, not a superposition. In the classical work of Timoshenko it is clear that the term "Superposition" refers to the superimposing of two or more solutions to distinct physical problems, static or dynamic, one-upon-the-other, and constraining them in such a way that a solution to the basic problem of interest may be achieved. This is not what is done in the method employed by Du, et al. Their method does, however, appear to give results in good agreement with previously published data for the case of plates with classical boundary conditions. The amount of computation work required in applying their method, appears nevertheless, to be massive and far exceeds that required by others investigating problems in the same area. The computational procedures outlined in two extensive appendices as well as in the main body of the paper are required to apply their method.

The authors were apparently unaware at the time of writing, of an existing publication in the literature resolving the problem of free in-plane vibration of rectangular plates with elastic support normal to the plate edges. A solution was obtained in the earlier publication by a much more concise approach employing the method of superposition [4].

The object of the present paper is to extend the superposition method to the analysis of in-plane free vibration of orthotropic rectangular plates. Attention is focused on plates where the principal directions of orthotropy co-inside with directions along the rectangular plate edges. For illustrative purposes the analysis described here is restricted to in-plane vibration of the fully clamped plate. It will be seen, however, that the method described can be extended to analyze the free vibration of rectangular plates with other combinations of classical boundary conditions.

A limited number of plate in-plane free vibration mode shapes are provided in the present paper. In addition, computed eigenvalues are tabulated for a limited number of plate geometries and orthotropic plate elastic properties. It is hoped that these results will provide data against which the findings of other researchers may be compared.

2. Mathematical procedure

2.1. The free vibration mode families

It will be obvious that free in-plane vibration mode displacements for the fully clamped rectangular plate will possess a certain amount of symmetry with respect to the plate central axes. We say that a mode possesses symmetry with respect to a central axis if displacements along the axis are everywhere zero and displacements perpendicular to the axis pass through a maximum along this same axis. Conversely, a mode is said to possess anti-symmetry with respect to an axis if displacements normal to the axis are everywhere zero and displacements parallel to the axis reach a maximum along this same axis. These definitions are discussed in detail in Ref. [2].

We therefore anticipate three distinct families of mode shapes. These are, symmetric-symmetric modes which possess symmetry with respect to each central axis, anti-symmetric–anti-symmetric modes which possess anti-symmetry with respect to each axis, and symmetric–anti-symmetric modes which possess symmetry with respect to one axis and anti-symmetry with respect to the other.

In what is to follow we will continue with the practice of analyzing each family of modes separately. As will be seen, this leads to a complete delineation between the mode families and helps simplify the mathematical treatment of the problem.

2.2. Development of non-dimensional equilibrium equations

Utilizing the coordinate system of Fig. 1 and the list of symbols as provided in the nomenclature the basic equilibrium equations are written as

$$\frac{\partial \sigma_x}{\partial x}+\frac{\partial \tau_{xy}}{\partial y}=\rho\frac{\partial^2 u}{\partial t^2}, \tag{1}$$

and

$$\frac{\partial \tau_{xy}}{\partial x}+\frac{\partial \sigma_y}{\partial y}=\rho\frac{\partial^2 v}{\partial t^2}. \tag{2}$$

The stress–strain relationships for orthotropic plate in-plane normal stresses are reviewed in Ref. [6], for example, and are as follows:

$$\sigma_x=\frac{E_x}{(1-\nu_x\nu_y)}[\varepsilon_x+\nu_y\varepsilon_y] \quad \text{and} \quad \sigma_y=\frac{E_y}{(1-\nu_x\nu_y)}[\varepsilon_y+\nu_x\varepsilon_x], \tag{3a,b}$$

while the shear stress–displacement relationship is

$$\tau_{xy}=G_{xy}\left[\frac{\partial v}{\partial x}+\frac{\partial u}{\partial y}\right]. \tag{3c}$$

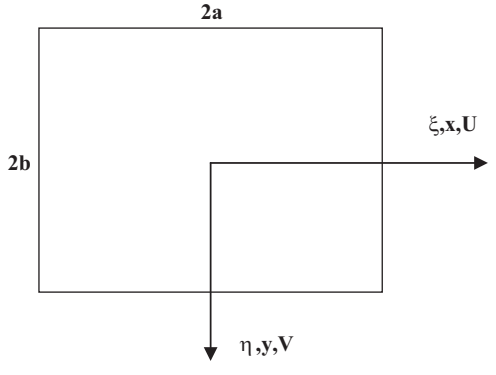

Fig. 1. Rectangular plate with central axes.

Introducing the strain–displacement relationships the above expressions for σ_x and σ_y become,

$$\sigma_x = A_{11}\frac{\partial u}{\partial x} + A_{12}\frac{\partial v}{\partial y} \quad \text{and} \quad \sigma_y = A_{22}\frac{\partial v}{\partial y} + A_{21}\frac{\partial u}{\partial x}, \tag{4a,b}$$

where

$$A_{11} = \frac{E_x}{1-\nu_x\nu_y}; \quad A_{12} = \frac{\nu_y E_x}{1-\nu_x\nu_y}; \quad A_{22} = \frac{E_y}{1-\nu_x\nu_y} \quad \text{and} \quad A_{21} = \frac{\nu_x E_y}{1-\nu_x\nu_y}. \tag{5a–d}$$

In view of the Betti Principle the product $\nu_y E_x = \nu_x E_y$, therefore $A_{12} = A_{21}$.

Returning to Eqs. (1) and (2), and introducing the stress–displacement relationships for normal and shear stresses we obtain

$$A_{11}\frac{\partial^2 u}{\partial x^2} + A_{12}\frac{\partial^2 v}{\partial x\partial y} + A_{66}\left\{\frac{\partial^2 v}{\partial x\partial y} + \frac{\partial^2 u}{\partial y^2}\right\} = \rho\frac{\partial^2 u}{\partial t^2}, \tag{6}$$

and

$$A_{66}\left\{\frac{\partial^2 v}{\partial x^2} + \frac{\partial^2 u}{\partial x\partial y}\right\} + A_{22}\frac{\partial^2 v}{\partial y^2} + A_{12}\frac{\partial^2 u}{\partial x\partial y} = \rho\frac{\partial^2 v}{\partial t^2}, \tag{7}$$

where $A_{66} = G_{xy}$.

Dividing displacements u and v by quarter plate edge length 'a', and coordinates x and y by quarter plate edge lengths 'a' and 'b', respectively, it is readily shown that the equilibrium Eqs. (6) and (7) may be written, respectively, as

$$\frac{\partial^2 U}{\partial\xi^2} + \frac{\nu_y}{\phi}\frac{\partial^2 V}{\partial\xi\partial\eta} + \frac{G(1-\nu_x\nu_y)}{E_x\phi}\left\{\frac{\partial^2 V}{\partial\xi\partial\eta} + \frac{1}{\phi}\frac{\partial^2 U}{\partial\eta^2}\right\} + \lambda^4 U = 0, \tag{8}$$

and

$$\frac{G_{xy}(1-\nu_x\nu_y)}{E_x}\left[\frac{\partial^2 V}{\partial\xi^2} + \frac{\partial^2 U}{\phi\partial\xi\partial\eta}\right] + \frac{E_y}{\phi^2 E_x}\frac{\partial^2 V}{\partial\eta^2} + \frac{\nu_y}{\phi}\frac{\partial^2 U}{\partial\xi\partial\eta} + \lambda^4 V = 0. \tag{9}$$

where $\lambda^2 = \omega a\sqrt{\rho(1-\nu_x\nu_y)/E_x}$.

Finally, the equilibrium Eqs. (8) and (9) may be written, respectively, in more compact form as

$$a_{11}\frac{\partial^2 U}{\partial\xi^2} + \frac{a_{12}}{\phi}\frac{\partial^2 V}{\partial\xi\partial\eta} + \frac{a_{66}}{\phi}\left\{\frac{\partial^2 V}{\partial\xi\partial\eta} + \frac{1}{\phi}\frac{\partial^2 U}{\partial\eta^2}\right\} + \lambda^4 U = 0, \tag{10}$$

and

$$a_{66}\left\{\frac{\partial^2 V}{\partial\xi^2} + \frac{1}{\phi}\frac{\partial^2 U}{\partial\xi\partial\eta}\right\} + \frac{a_{12}}{\phi}\frac{\partial^2 U}{\partial\xi\partial\eta} + \frac{a'_{11}}{\phi^2}\frac{\partial^2 V}{\partial\eta^2} + \lambda^4 V = 0, \tag{11}$$

where $a_{11} = 1$, $a_{12} = \nu_y$, $a_{66} = G_{xy}(1-\nu_x\nu_y)/E_x$ and $a'_{11} = E_y/E_x$.

Eqs. (10) and (11) are the dimensionless formulations of the equilibrium equations employed here for orthotropic plate in-plane free vibration analysis. In the limit as the orthotropic plate properties approach those of an isotropic plate it is found, as expected, that the above equilibrium equations approach those of the isotropic plate [2].

2.3. The in-plane normal and shear stresses in non-dimensional form

Utilizing expressions for the quantities σ_x and σ_y introduced earlier, we now introduce the dimensionless stress quantities,

$$\sigma_x^* = \frac{\sigma_x(1-\nu_x\nu_y)}{E_x} \quad \text{or} \quad \sigma_x^* = \frac{\partial U}{\partial\xi} + \frac{\nu_y}{\phi}\frac{\partial V}{\partial\eta}, \tag{12a,b}$$

and

$$\sigma_y^* = \frac{\sigma_y(1-v_x v_y)}{E_y} \quad \text{or} \quad \sigma_y^* = v_x \frac{\partial U}{\partial \xi} + \frac{1}{\phi}\frac{\partial V}{\partial \eta}. \tag{12c,d}$$

We also now introduce the dimensionless shear stress quantity,

$$\tau_{xy}^* = \frac{\tau_{xy}\phi}{G_{xy}} \quad \text{or} \quad \tau_{xy}^* = \frac{\partial U}{\partial \eta} + \phi \frac{\partial V}{\partial \xi}. \tag{12e,f}$$

2.4. The fully symmetric modes

The orthotropic rectangular plate of interest is shown schematically in Fig. 1. Taking advantage of symmetry we follow well established practices and analyze one quarter of the plate only, as shown on the left hand side of Fig. 2. Small circles adjacent to the ξ and η axes indicate lines of modal symmetry. Free vibration modes will have zero displacement along these axes. Displacements normal to the axes take on a maximum amplitude along these same axes.

Free vibration analysis of this family of modes is accomplished through superimposing solutions for the response of the two forced vibration problems (building blocks) shown schematically to the right of the figure. These building blocks are identical to those described earlier for analyzing fully symmetric modes of the fully clamped isotropic rectangular plate [3]. Only a brief description of the analytical procedure will be provided, therefore, for the sake of completeness. We begin by focusing attention on the first building block. A condition of zero displacement parallel to the edges $\xi = 1$, and $\eta = 1$, is imposed. The edge $\eta = 1$, is driven by a distributed harmonic normal stress of circular frequency ω and represented in the figure by short arrows. We represent amplitude of response of this building block with Levy type series as

$$U(\xi,\eta) = \sum_{m=1,2}^{\infty} U_m(\eta) \cos m\pi\xi, \tag{13}$$

and

$$V(\xi,\eta) = \sum_{m=1,2}^{\infty} V_m(\eta) \sin m\pi\xi. \tag{14}$$

It will be noted that each term in this Levy type solution satisfies exactly the required conditions of symmetry along the η axis, as well as zero displacement V along the edge, $\xi = 1$.

Following established practices Eqs. (13) and (14) are substituted into the equilibrium Eqs. (10) and (11) to obtain

$$a_{m1} U_m^{\|}(\eta) + b_{m1} V_m^{|}(\eta) + c_{m1} U_m(\eta) = 0, \tag{15}$$

and

$$a_{m2} V_m^{\|}(\eta) + b_{m2} U_m^{|}(\eta) + c_{m2} V_m(\eta) = 0, \tag{16}$$

where superscripts imply differentiation with respect to the variable, η, and

$$a_{m1} = \frac{a_{66}}{\phi^2}, \quad b_{m1} = \frac{\text{emp}}{\phi}(a_{12} + a_{66}), \quad c_{m1} = -a_{11}\text{emps} + \lambda^4, \tag{17a–c}$$

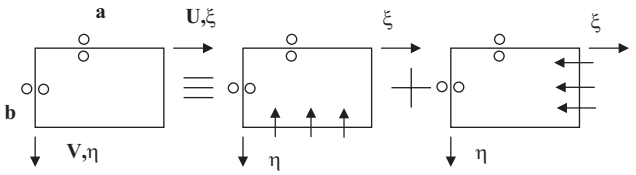

Fig. 2. Building blocks employed in analysis of symmetric–symmetric modes of fully clamped plate.

$$a_{m2} = a_{11}^{|}/\phi^2, \quad b_{m2} = -\frac{\text{emp}}{\phi}(a_{66} + a_{12}), \quad c_{m2} = -a_{66}\text{emps} + \lambda^4, \tag{18a–c}$$

here symbols emp and emps are introduced to represent the quantities $m\pi$, and $(m\pi)^2$, respectively. Note that the quantities a_{m1}, b_{m1}, etc., differ from those of the fully clamped isotropic plate, [3], only in that now quantity a_{m2} equals the ratio $(E_y/E_x)/\varphi^2$ instead of $1/\varphi^2$ (the isotropic case).

Exact solutions for the quantities $U_m(\eta)$ and $V_m(\eta)$ of Eqs. (15) and (16) were obtained in Ref. [3]. There is therefore no need to describe the solution procedure in detail here. Only a brief description of the steps involved is provided for completeness.

By manipulation of Eqs. (15) and (16) through addition and subtraction the quantity $V_m(\eta)$ is isolated in order to obtain the fourth order ordinary homogeneous differential equation

$$V_m^{\text{IV}}(\eta) + bV_m^{\|}(\eta) + cV_m(\eta) = 0, \tag{19}$$

where $b = (a_{m1}c_{m2} - b_{m1}b_{m2} + c_{m1}a_{m2})/a_{m1}a_{m2}$ and $c = c_{m1}c_{m2}/a_{m1}a_{m2}$.

Again, superscripts indicate the order of differentiation with respect to η.

The squares of the roots of the characteristic equation associated with Eq. (19) are

$$\varepsilon_1^2 = \frac{-b + \sqrt{b^2 - 4c}}{2} \quad \text{and} \quad \varepsilon_2^2 = \frac{-b - \sqrt{b^2 - 4c}}{2}. \tag{20a,b}$$

Consider first the forms of solution applicable for Eq. (19) when the quantity $b^2 - 4c \geqslant 0$. This latter condition has always been found to hold when analyzing isotropic plates. The quantities ε_1^2 and ε_2^2 will then always be real though they could be positive or negative. In Ref. [3] we designated these quantities Root1 and Root2, respectively. We also introduced the quantities,

$$\beta_m = \sqrt{|\text{Root1}|} \quad \text{and} \quad \gamma_m = \sqrt{|\text{Root2}|}. \tag{21a,b}$$

Three possible forms of solution for Eq. (19) were shown to exist. They are:

Solution 1: Root1 $\geqslant 0$, Root2 $\leqslant 0$, then

$$V_m(\eta) = A_m \sinh \beta_m\eta + B_m \cosh \beta_m\eta + C_m \sin \gamma_m\eta + D_m \cos \gamma_m\eta. \tag{22}$$

Solution 2: Root1 $\leqslant 0$, Root2 $\leqslant 0$,

$$V_m(\eta) = A_m \sin \beta_m\eta + B_m \cos \beta_m\eta + C_m \sin \gamma_m\eta + D_m \cos \gamma_m\eta. \tag{23}$$

Solution 3: Root1 $\geqslant 0$, Root2 $\geqslant 0$,

$$V_m(\eta) = A_m \sinh \beta_m\eta + B_m \cosh \beta_m\eta + C_m \sinh \gamma_m\eta + D_m \cosh \gamma_m\eta. \tag{24}$$

The quantities A_m, B_m, etc., are constants to be evaluated according to the boundary conditions to be enforced.

Before establishing the quantity $V_m(\eta)$ one further significant step is required. It is found that for orthotropic plates the quantity, $b^2 - 4c$, discussed above, is not necessarily positive. In fact, this is the main difference encountered in moving from isotropic to orthotropic plates. Accordingly, we must formulate the correct known solution for this special case. To achieve this end we set up the following quantities,

$$zz1 = -b/2, \quad zz2 = \sqrt{-(b^2 - 4c)}/2, \quad zz3 = \tan^{-1}(zz2/zz1), \quad zz4 = \{zz1^2 + zz2^2\}^{1/4}, \tag{25a–d}$$

with

$$R = zz4 \sin(zz3/2) \quad \text{and} \quad S = zz4 \cos(zz3/2). \tag{25e,f}$$

The solution for the quantity $V_m(\eta)$ then becomes,

$$V_m(\eta) = A_m \sin R\eta \sinh S\eta + B_m \sin R\eta \cosh S\eta + C_m \cos R\eta \sinh S\eta + D_m \cos R\eta \cosh S\eta. \tag{26}$$

We will refer to this as Solution 4.

With solution for the quantity $V_m(\eta)$ available for any problem of interest we turn to evaluation of the companion quantity $U_m(\eta)$. It is readily shown that through manipulation of the equilibrium Eqs. (15)

and (16), we can express the quantity $U_m(\eta)$ in terms of the derivatives of the quantity $V_m(\eta)$ as follows [3]:

$$U_m(\eta) = \frac{a_{m1}a_{m2}}{c_{m1}b_{m2}} V_m^{|||}(\eta) + \left[\frac{a_{m1}c_{m2} - b_{m1}b_{m2}}{c_{m1}b_{m2}}\right] V_m^{|}(\eta). \tag{27}$$

Details of this mathematical operation as it applies to the first three forms of the solution, $(b^2-4c)\geqslant 0$, are provided in Ref. [3]. The same procedure is followed for the solution with $(b^2-4c)\leqslant 0$.

The next step is to evaluate the constants appearing in these solutions utilizing the prescribed boundary conditions. It will be obvious that for fully symmetric mode vibration analytical terms appearing in the quantity $V_m(\eta)$ which are anti-symmetric with respect to the ξ axis must be deleted. This eliminates two of the four constants which appear in the four solution forms.

A third boundary condition to be enforced is the requirement of zero displacement parallel to the driven edge, $\eta = 1$. Details related to enforcement of this boundary condition for the first three solution forms are provided in Ref. [3]. An identical procedure is followed in connection with the fourth solution form, however, it is cautioned that because of the existence of products of trigonometric and hyperbolic functions in this latter solution the operation of taking derivatives of the quantities $V_m(\eta)$ and $U_m(\eta)$ will be considerably more laborious. After deleting terms anti-symmetric about the ξ axis for this latter solution, and enforcing the third boundary condition as described above, the quantity $V_m(\eta)$ will have taken on the form,

$$V_m(\eta) = A_m\{\sin\ R\eta\ \sinh\ S\eta + \theta_{1m}\ \cos\ \eta\ \cosh\ S\eta\}. \tag{28}$$

Finally, we must evaluate the last unknown appearing in those solution forms through enforcement of dynamic equilibrium between the local normal stress and the imposed driving stress along the driven edge. Amplitude of this distributed driving stress is expressed in series form, for the fully symmetric mode study as

$$\sigma_y^*|_{\eta=1} = \sum_{m=1,2}^{\infty} E_m\ \sin\ \mathrm{emp}\xi. \tag{29}$$

This edge condition is easily enforced. It is shown, for example, in Ref. [3] that the solution for $V_m(\eta)$ related to the first form of solution is written as

$$V_m(\eta) = E_m\theta_{11m}[\cosh\ \beta_m\eta + \theta_{1m}\ \cos\ \gamma_m\eta], \tag{30}$$

with companion solution $U_m(\eta)$ given as

$$U_m(\eta) = E_m\theta_{11m}[\alpha_{2m}\ \sinh\ \beta_m\eta + \theta_{1m}\alpha_{4m}\ \sin\ \gamma_m\eta], \tag{31}$$

where expressions for θ_{11m}, θ_{1m}, α_{2m} etc., are to be found in the reference. Corresponding expressions also are given for these displacements as they relate to the second and third solution forms.

Solution for the same quantities related to the fourth form of solution is obtained in an identical fashion but the quantities θ_{1m} and θ_{11m} will be more complicated because of the presence of products of trigonometric and hyperbolic functions as discussed above. In the present work it is shown that for the fourth form of solution we obtain

$$V_m(\eta) = E_m\theta_{11m}[\sin\ R\eta\ \sinh\ S\eta + \theta_{1m}\ \cos\ R\eta\ \cosh\ S\eta], \tag{32}$$

and

$$\begin{aligned} U_m(\eta) = {} & E_m\theta_{11m}[RR1\ \sin\ R\eta\ \cosh\ S\eta + RR2\ \cos\ R\eta\ \cosh\ S\eta] \\ & + E_m\theta_{11m}\theta_{1m}[RR3\ \cos\ R\eta\ \sinh\ S\eta + RR4\ \sin\ R\eta\ \cosh\ S\eta], \end{aligned} \tag{33}$$

where quantities θ_{11m}, θ_{1m}, $RR1, RR2$, etc., must be evaluated.

It is important to note that we now have available the response of any force driven orthotropic building block as discussed above to any distributed harmonic normal stress enforced along the driven edge.

We turn next to determining the response of the second building block of Fig. 2. It differs from the first in that it is driven along the edge, $\xi = 1$, with conditions of zero displacement parallel to this edge. A condition of zero motion parallel to the edge, $\eta = 1$, is also imposed. The second building block is essentially a mirror image of the first and it will be apparent that its solution can be obtained through a transformation of that already developed for the first [3]. A proper interchange of axes is required. Certain rules must be followed in

performing this axis interchange and it will be seen that they are slightly more complicated than those related to isotropic plates. We still wish to use the symbols U and V to indicate displacement parallel to the ξ and η axes, respectively. After interchange of the variables ξ and η we write for response of the second building block (see Eqs. (13) and (14)),

$$U(\xi,\eta)=\sum_{n=1,2}^{\infty} U_n(\xi)\sin n\pi\eta, \tag{34}$$

and

$$V(\xi,\eta)=\sum_{n=1,2}^{\infty} V_n(\xi)\cos n\pi\eta, \tag{35}$$

where the subscript 'n' is used in order to avoid confusion with solution for the first building block. Here, in the interest of brevity we may introduce the symbols $\mathrm{enp}=n\pi$, with $\mathrm{enps}=\mathrm{enp}^2$. In order to obtain the solution for this second building block we must make the following temporary changes, in this order:

(1) replace λ^2 with the quantity $\lambda^2\varphi\sqrt{E_x/E_y}$;
(2) replace φ with its inverse $1/\varphi$;
(3) referring to quantities a_{11}, a_{22}, etc., following Eq. (11), set $a_{12}=v_x$, and replace A_{66} with $A_{66}\,E_x/E_y$; and
(4) we now denote the quantities a_{m1}, b_{m1} etc., of Eqs. (15) and (16) by the symbols a_{n1}, b_{n1}, etc., and enp and enps will replace emp and emps. a_{n2} now becomes $(E_x/E_y)/\phi^2$.

These new quantities permit evaluation of β_n and γ_n, replacing β_m and γ_m of the first three forms of solution for the first building block. Quantities R and S associated with the fourth solution are also evaluated as was done for the first building block. Quantities θ_{1n} and θ_{11n}, etc., for each of the four forms of solution are extracted from quantities θ_{1m} and θ_{11m}, etc., of the previous solution by simply replacing the quantities β_m, γ_m, etc., with the new quantities β_n, γ_n, etc.

This completes obtaining of the solution for response of the second building block of Fig. 2. It is shown that this latter solution is obtained through an orderly transformation of the solution provided for the first. Before discussing generation of the eigenvalue matrix for the obtaining of eigenvalues and mode shapes for free vibration of any mode family of interest we will first introduce solutions for the building blocks related to the fully anti-symmetric and symmetric–anti-symmetric mode families of orthotropic plates.

2.5. The fully anti-symmetric modes

The quarter plate associated with this family of modes is shown schematically on the left hand side of Fig. 3. Displacements are anti-symmetric with respect to both the ξ and η axes. Analysis of this family of modes is accomplished by means of the two building blocks shown to the right of the figure. They will each, of course, satisfy the same anti-symmetric mode conditions along the axes.

Driven edges of the building blocks again have zero displacement parallel to these edges. The same edges are subjected to a distributed harmonic normal driving stress. Non-driven outer edges have zero displacement parallel to these edges.

The mathematical procedure followed in analyzing this family of modes differs very little from that described for the fully symmetric mode family. Only these differences will be elaborated upon. In order to

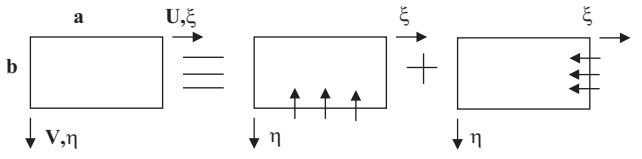

Fig. 3. Building blocks employed in analysis of fully anti-symmetric modes of fully clamped plate.

satisfy the new boundary conditions we now represent the displacements of the first building block as

$$U(\xi,\eta)=\sum_{m=1,2}^{\infty}U_m(\eta)\sin(2m-1)\pi\xi/2, \tag{36}$$

and

$$V(\xi,\eta)=\sum_{m=1,2}^{\infty}V_m(\eta)\cos(2m-1)\pi\xi/2. \tag{37}$$

Substituting these displacement expressions in the equilibrium equations we again obtain Eqs. (15) and (16) where now

$$a_{m1}=\frac{a_{66}}{\varphi^2},\quad b_{m1}=-\frac{\mathrm{emp}}{\varphi}[a_{12}+a_{66}],\quad c_{m1}=-a_{11}\mathrm{emps}+\lambda^4, \tag{38a-c}$$

and

$$a_{m2}=\frac{a_{11}^{|}}{\varphi^2},\quad b_{m2}=\frac{\mathrm{emp}}{\varphi}[a_{66}+a_{12}]\quad\text{and}\quad c_{m2}=-a_{66}\mathrm{emps}+\lambda^4. \tag{39a-c}$$

Here, emp $=(2m-1)\pi/2$, and emps $=\mathrm{emp}^2$. The symbols a_{11}, a_{12}, a_{66}, and $a_{11}^{|}$, are as defined earlier following Eq. (11).

Again, the ordinary differential Eq. (19) and its solution forms are applicable, the only difference being that the coefficients will be changed. β_m and γ_m related to the first three solution forms are now available as well as quantities R and S related to the fourth solution form. The major difference is that now for the quantities $V_m(\eta)$ we must delete terms symmetric with respect to the ξ axis. Deleting these terms and enforcing the applicable boundary conditions along the driven edge we now obtain for the first form of solution, for example,

$$V_m(\eta)=E_m\theta_{11m}[\sinh\,\beta_m\eta+\theta_{1m}\,\sin\,\gamma_m\eta], \tag{40}$$

with

$$U_m(\eta)=E_m\theta_{11m}[\alpha_{1m}\,\cosh\,\beta_m\eta+\theta_{1m}\,\cos\,\gamma_m\eta], \tag{41}$$

again, with quantities θ_{11m} etc., available from Ref. [3]. The fourth form of solution will be written as

$$V_m(\eta)=E_m\theta_{11m}[\sin\,R\eta\,\cosh\,S\eta+\theta_{1m}\,\cos\,R\eta\,\sinh\,S\eta], \tag{42}$$

with

$$U_m(\eta)=E_m\theta_{11m},[RR1\,\sin\,R\eta\,\sinh\,S\eta+RR2\,\cos\,R\eta\,\cosh\,S\eta], \tag{43}$$

where for this solution, quantities θ_{11m}, θ_{1m}, $RR1$, etc., must be evaluated.

A solution for response of the second building block of Fig. 4 is obtained through a transformation of the first building block solution following rules of transformation provided in detail earlier.

2.6. The symmetric–anti-symmetric modes

The quarter plate associated with this family of modes is shown schematically on the left hand side of Fig. 4. Displacements are symmetric with respect to the ξ axis and anti-symmetric with respect to the η axis. Analysis

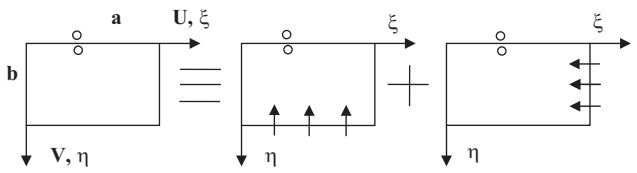

Fig. 4. Building blocks employed in analyzing symmetric–anti-symmetric modes of fully clamped plate.

of this family of modes is accomplished by means of the two building blocks shown to the right of the figure. They each must satisfy the required boundary conditions along the respective axes. These building blocks have also been described in Ref. [3] so only a brief description is provided here.

The in-plane displacements U and V of the first building block will be given by Eqs. (36) and (37) related to the first building block of the fully anti-symmetric mode study. Quantities a_{m1}, b_{m1}, etc., will be identical to those provided for the earlier study. The only difference in obtaining solution to response of the first building block is that now terms for displacement V, anti-symmetric about the ξ axis, must be deleted. Enforcing appropriate boundary conditions along the driven edge one solves for the quantities U and V for all possible solution forms. Solutions for the first three forms are available in Ref. [3]. Solutions of the first form are as given by Eqs. (30) and (31) with the parameters θ_{1m} and θ_{11m} as provided in the reference. The form of the fourth solution will be identical to that given by Eqs. (32) and (33). Of course, the related quantities θ_{1m}, θ_{11m}, $RR1$, etc., must be computed.

It is obvious that solution for response of the second building block of Fig. 4 cannot be extracted from that of the first. The problem was addressed in Ref. [3]. The procedure adopted was to first obtain a solution for response of the building block of Fig. 5. Solution for the second building block of Fig. 4 can then be extracted from this latter solution through an interchange of axes.

It is seen that solution for the building block of Fig. 5 differs only slightly from that of the first building block employed earlier in the symmetric–symmetric mode study. The single difference lies in the fact that terms symmetric about the ξ axis must be deleted when evaluating the quantity $V(\xi,\eta)$. This has in fact been done for the first three forms of solution, ($b^2-4c\geqslant 0$), in Ref. [3] and is not repeated here. The first form of solution will be expressed according to Eqs. (40) and (41) with quantities θ_{1m}, and θ_{11m} available from Ref. [3]. The fourth solution will take the form given by Eqs. (42) and (43), where again the quantities θ_{1m}, θ_{11m}, $RR1$, etc., must be computed.

Finally it will be evident that solution for the second building block of Fig. 4 is readily extracted from that given immediately above through transformation of the axes. This completes development of all building block solutions required for the free in-plane vibration analysis of the fully clamped orthotropic plate.

2.7. Development of eigenvalue matricies

Generation of this matrix for clamped isotropic plates is described in detail in Ref. [3]. Since the process for generation of the matrix for orthotropic plates is essentially identical, only a very brief description is given here.

Concentrating on the two building blocks employed in the symmetric–symmetric mode study, for illustrative purposes, we recognize that solutions for these respective building blocks must be superimposed, one-upon-the-other, and their driving coefficients, E_m and E_n must be constrained so as to satisfy the condition of zero net displacement perpendicular to the quarter plate outer edges. This is achieved by first expanding the contributions of each building block to displacement along these edges in an appropriate trigonometric series. By utilizing the sine series of Eq. (14) we find that a series expansion of the first building block contribution to

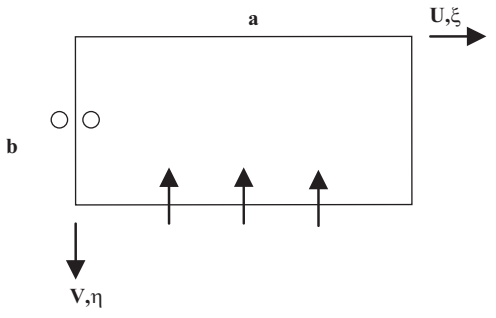

Fig. 5. Intermediate building block utilized in analyzing symmetric–anti-symmetric modes of fully clamped plate.

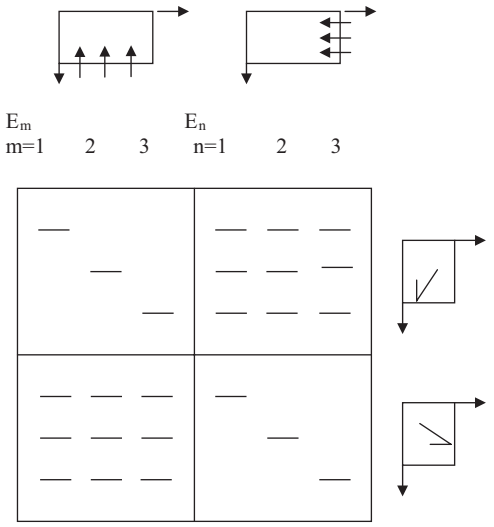

Fig. 6. Schematic representation of eigenvalue matrix based on 3-term building block solutions.

displacement along the edge, $\eta = 1$, already exists. Contributions of the second building block toward this same displacement are expanded in the same series following standard procedures. We thus arrive at a set of K linear homogeneous algebraic equations relating the $2K$ driving coefficients, where K equals the number of terms utilized in the building block solutions.

A corresponding set of K equations is obtained through imposing the condition of zero net displacement normal to the edge, $\xi = 1$. We thus arrive at a set of $2K$ homogeneous algebraic equations relating the $2K$ unknown driving coefficients. Eigenvalues are those values of the parameter λ^2 which cause the determinant of the coefficient matrix of these equations (the eigenvalue matrix) to vanish. A schematic representation of this eigenvalue matrix, based on three term building block solutions, is presented in Fig. 6.

With eigenvalues established, one of the non-zero driving coefficients is set equal to unity, thereby permitting establishment of the mode shape associated with any eigenvalue. Solutions for eigenvalues and mode shapes for the remaining two mode families are obtained in an identical fashion.

3. Presentation of computed results

3.1. Selection of input parameters

There are, of course, an infinite number of input parameter combinations which could be utilized in orthotropic plate analysis. For illustrative purposes a particular set of such values was utilized in the work reported here.

First we select a value for the stiffness ratio E_y/E_x. We choose to consider the product $v_y v_x$ to equal v^2, where v is the Poisson ratio for isotropic materials and is taken here to equal 0.3. This permits immediate evaluation of v_y and v_x whose ratio v_y/v_x must equal E_y/E_x. Finally, we must assign a value to G_{xy}, the modulus of elasticity in shear for the orthotropic material. It is suggested by Zillard [7], that a reasonable formulation for this parameter is given by the ratio $[E_x E_y]^{1/2}/2(1+v_x v_y)$. In particular, we will be interested in formulation of the quantity $a_{66} = G_{xy}/E_x(1-v_x v_y)$, introduced earlier. It follows, therefore, that we may write

$$a_{66} = \left[\frac{E_y}{E_x}\right]^{1/2} \left\{\frac{1 - v_x v_y}{2(1 + [v_x v_y]^{1/2})}\right\}. \tag{44}$$

It is noted that as the ratio E_y/E_x approaches unity all parameters return to those of the isotropic plate.

3.2. Tabulation of computed eigenvalues

For each of the three mode families studied, eigenvalues have been computed and tabulated with the stiffness ratio E_y/E_x taking on values of 1.0, 1.25, 1.5, 2.0, and 2.5. Plate aspect ratios take on values of 1.0, 1.25, 1.5, and 2.0, as well as the inverse of these values. In the case of symmetric–anti-symmetric mode studies results are also tabulated for plates with ratios E_y/E_x equal to the inverse of those given above. This is necessary because of the lack of symmetry encountered when analyzing symmetric–anti-symmetric modes. These computed eigenvalues are to be found in Tables 1–4.

It will be noted that eigenvalues are tabulated to four significant digits. Numerous convergence studies were conducted before selecting a value of K, the number of terms employed in the building block solutions. It was concluded that a value of K equal to 9 would assure four digit accuracy in computed results. This is the value of K employed in computing all results reported here.

Table 1
Fully symmetric mode eigenvalues.

Mode	E_y/E_x				
	1.0	1.25	1.5	2.0	2.5
$\phi = 1.0$					
(1)	2.118	2.235	2.332	2.488	2.611
(2)	2.593	2.738	2.882	3.142	3.371
(3)	3.798	4.010	4.182	4.442	4.608
$\phi = 1.25$					
(1)	1.918	1.999	2.067	2.175	2.256
(2)	2.347	2.483	2.613	2.844	3.046
(3)	3.164	3.337	3.480	3.721	3.917
$\phi = 1.5$					
(1)	1.801	1.860	1.910	1.962	2.027
(2)	2.201	2.331	2.451	2.663	2.845
(3)	2.733	2.874	2.990	3.187	3.349
$\phi = 2.0$					
(1)	1.678	1.714	1.702	1.750	1.790
(2)	2.035	2.154	2.259	2.434	2.576
(3)	2.249	2.347	2.453	2.587	2.721
$\phi = 1.0/1.25$					
(1)	2.397	2.562	2.700	2.918	3.088
(2)	2.934	3.104	3.255	3.550	3.811
(3)	3.954	4.183	4.370	4.661	4.882
$\phi = 1.0/1.5$					
(1)	2.701	2.914	3.093	3.376	3.596
(2)	3.301	3.490	3.669	3.986	4.279
V(3)	4.100	4.353	4.567	4.911	5.187
$\phi = 1.0/2.0$					
(1)	3.356	3.663	3.926	4.345	4.663
(2)	4.070	4.305	4.515	4.899	5.240
(3)	4.499	4.815	5.090	5.560	5.964

Table 2
Fully anti-symmetric mode eigenvalues.

Mode	E_y/E_x				
	1.0	1.25	1.5	2.0	2.5
$\phi = 1.0$					
(1)	2.929	3.056	3.118	3.181	3.219
(2)	3.354	3.563	3.745	4.012	4.207
(3)	3.641	3.876	4.127	4.634	5.094
$\phi = 1.25$					
(1)	2.524	2.746	2.901	3.054	3.114
(2)	3.107	3.219	3.319	3.521	3.648
(3)	3.337	3.460	3.599	3.912	4.251
$\phi = 1.5$					
(1)	2.188	2.404	2.586	2.850	2.992
(2)	2.981	3.095	3.166	3.270	3.379
(3)	3.197	3.263	3.342	3.527	3.741
$\phi = 2.0$					
(1)	1.762	1.936	2.090	2.352	2.566
(2)	2.813	2.939	3.027	3.133	3.176
(3)	2.936	3.062	3.119	3.193	3.288
$\phi = 1.0/1.25$					
(1)	3.155	3.212	3.250	3.304	3.345
(2)	3.884	4.156	4.364	4.680	4.924
(3)	4.171	4.553	4.914	5.482	5.782
$\phi = 1.0/1.5$					
(1)	3.282	3.332	3.372	3.434	3.485
(2)	4.472	4.775	5.016	5.391	5.683
(3)	4.479	5.249	5.575	5.916	6.078
$\phi = 1.0/2.0$					
(1)	3.524	3.588	3.643	3.736	3.814
(2)	5.627	5.938	6.112	6.283	6.377
(3)	5.872	6.192	6.466	6.939	7.327

Accurate results were not found available in the literature for the purposes of comparison. A number of tests and procedures were therefore employed to help verify the present results. First, extensive maps of eigenvalues vs. input stiffness ratios, E_y/E_x, were generated. Even though results were tabulated for only a limited number of discrete points on these maps, continuity of eigenvalue curves was thereby demonstrated for each plate aspect ratio and this helped assure that no eigenvalues were missed.

Another demanding test was imposed on the computational scheme for various combinations of plate aspect ratios and stiffness ratios, E_y/E_x. Consider, for example, the first fully symmetric mode eigenvalue for a plate with both aspect ratio and ratio E_y/E_x greater than one. If we next conduct the same analysis with both of these parameters taking on their inverse ratios it will be appreciated that we must obtain identical free vibration frequencies, though not necessarily the same eigenvalue. This same test was applied to fully anti-symmetric mode studies. In every case studied exact frequency agreement was obtained.

Table 3
Symmetric–anti-symmetric mode eigenvalues with stiffness ratio $E_y/E_x \geqslant 1.0$.

Mode	E_y/E_x				
	1.0	1.25	1.5	2.0	2.5
$\phi = 1.0$					
(1)	1.778	1.957	2.118	2.399	2.643
(2)	2.947	3.100	3.222	3.405	3.544
(3)	3.557	3.713	3.856	4.119	4.358
$\phi = 1.25$					
(1)	1.526	1.672	1.802	2.032	2.231
(2)	2.850	2.982	3.081	3.220	3.320
(3)	3.245	3.417	3.562	3.814	4.036
$\phi = 1.5$					
(1)	1.371	1.994	1.605	1.800	1.969
(2)	2.786	2.910	2.999	3.116	3.195
(3)	2.968	3.173	3.332	3.583	3.782
$\phi = 2.0$					
(1)	1.197	1.295	1.382	1.535	1.667
(2)	2.379	2.592	2.752	2.940	3.034
(3)	2.799	2.939	3.054	3.341	3.380
$\phi = 1.0/1.25$					
(1)	2.113	2.335	2.533	2.880	3.174
(2)	3.107	3.293	3.447	3.692	3.890
(3)	3.889	4.056	4.211	4.499	4.761
$\phi = 1.0/1.5$					
(1)	2.463	2.727	2.964	3.372	3.710
(2)	3.308	3.531	3.721	4.035	4.300
(3)	4.214	4.401	4.574	4.892	5.178
$\phi = 1.0/2.0$					
(1)	3.189	3.540	3.850	4.371	4.778
(2)	3.804	4.111	4.379	4.845	5.266
(3)	4.858	5.100	5.315	5.699	6.035

3.3. Some mode shape studies

A limited number of mode shape studies were conducted. The objectives were to illustrate the effects of plate orthotropy on these mode shapes as well as to confirm that the expected trends in these shapes, away from shapes related to isotropic plates, were exhibited.

The first fully symmetric mode of a square plate with stiffness ratio E_y/E_x equal 1.0 (the isotropic case) is depicted in Fig. 7. In all mode shapes depicted here displacements within the quarter plate, only, are shown.

It is seen that conditions of zero displacement both parallel and normal to the plate outer edges are satisfied. These conditions will be seen to be satisfied in all mode shapes presented here. Conditions of zero displacement along the plate central axes are also noted. This is a requirement for fully symmetric modes. We note that displacements normal to these axes are equal along each axis. This is to be expected for the isotropic plate.

The first fully symmetric mode of a square plate with Young's moduli ratio equal to 2.0 is depicted in Fig. 8. Displacements along the outer plate edges and plate central axes are seen to be similar to those of Fig. 7 except

Table 4
Symmetric–anti-symmetric mode eigenvalues with stiffness ratio $E_y/E_x \leqslant 1.0$.

Mode	E_x/E_y				
	1.0	1.25	1.5	2.0	2.5
$\phi = 1.0$					
(1)	1.778	1.612	1.388	1.237	1.131
(2)	2.947	2.791	2.663	2.471	2.329
(3)	3.557	3.406	3.278	2.970	2.731
$\phi = 1.25$					
(1)	1.526	1.390	1.293	1.076	0.9923
(2)	2.850	2.710	2.594	2.378	2.195
(3)	3.245	3.061	2.891	2.595	2.297
$\phi = 1.5$					
(1)	1.371	1.254	1.171	0.9846	0.9133
(2)	2.786	2.642	2.494	2.222	2.015
(3)	2.968	2.753	2.594	2.399	2.265
$\phi = 2.0$					
(1)	1.197	1.102	1.036	0.9411	0.8750
(2)	2.379	2.165	1.990	1.755	1.591
(3)	2.799	2.658	2.544	2.370	2.201
$\phi = 1.0/1.25$					
(1)	2.113	1.909	1.657	1.464	1.330
(2)	3.107	2.923	2.780	2.565	2.409
(3)	3.889	3.737	3.620	3.431	3.257
$\phi = 1.0/1.5$					
(1)	2.463	2.221	1.946	1.710	1.547
(2)	3.308	3.092	2.927	2.684	2.510
(3)	4.214	4.047	3.918	3.729	3.578
$\phi = 1.0/2.0$					
(1)	3.189	2.870	2.555	2.232	2.009
(2)	3.804	3.815	3.300	2.952	2.739
(3)	4.858	4.633	4.456	3.961	3.378

for one consideration. It will be noted that displacements normal to the ξ axis are significantly lower than those normal to the η axis. This is to be anticipated since, with the Young's modulus ratio equal to 2.0, the plate is much stiffer in the η direction than in the ξ direction. This is visual evidence of the role orthotropy plays in determining the plate in-plane free vibration mode shapes. It also attests to the validity of the theoretical model.

Corresponding mode shapes for the first fully anti-symmetric mode vibration of a square plate are presented in Figs. 9 and 10. In Fig. 9 it is seen that displacements normal to the axes and normal to the quarter plate outer edges are everywhere zero, as required. While displacements parallel to the plate outer edges are everywhere zero, displacements parallel to the axes, at points located along these axes, are seen to be non-zero. This is why horizontal and vertical lines in the figure, with the exception of those lying along the above mentioned axes or plate outer edges, exhibit a distinct curvature, the degree of curvature being approximately equal for corresponding horizontal and vertical lines.

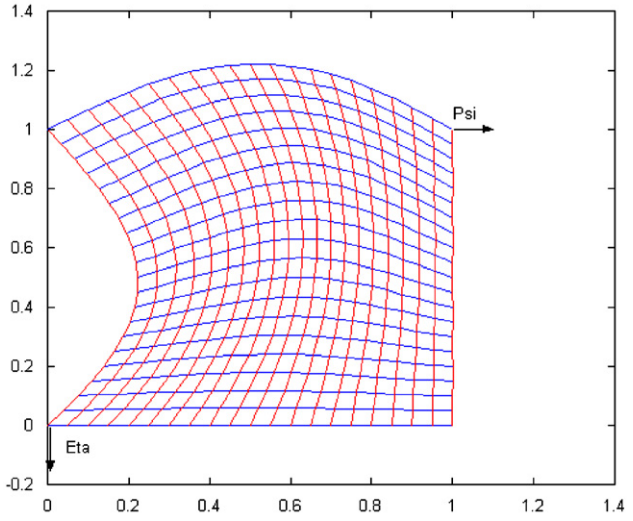

Fig. 7. First fully symmetric mode for square plate: stiffness ratio = 1.0.

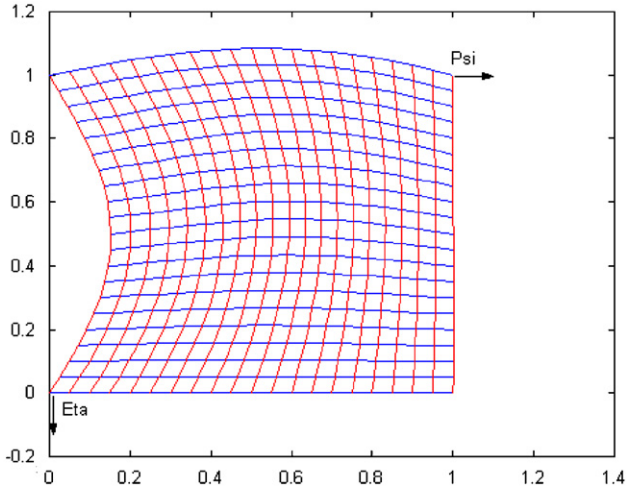

Fig. 8. First fully symmetric mode for square plate: stiffness ratio = 2.0.

Turning to Fig. 10 it is observed that similar conditions prevail, however, vertical lines in the figure have much higher curvature than corresponding horizontal lines. This is because with a stiffness ratio equal to 2.0 there is less stiffness in the ξ direction than in the η direction. There is thus less resistance to horizontal movement along the ξ axis than there is to vertical movement along the η axis. This results in the higher degree of curvature observed along the vertical lines as noted above.

In Figs. 11 and 12 first symmetric–anti-symmetric modes are depicted for the square plate. Conditions of symmetry, as described earlier, are imposed along the ξ axis. It will be noted that approximately equal amplitude of displacement normal to the ξ axis are observed in each figure. The degree of curvature observed in corresponding vertical lines of each figure are, however, considerably different. Examining the seventh vertical line from the edge, $\xi = 1$, of each figure, we note that the vertical line of Fig. 12 has almost twice as high a degree of curvature as that of Fig. 11. Again, this is a result of the lower plate stiffness in the ξ direction in Fig. 12 (stiffness ratio $E_y/E_x = 2.$), thereby making horizontal movement for this latter plate more easily achieved.

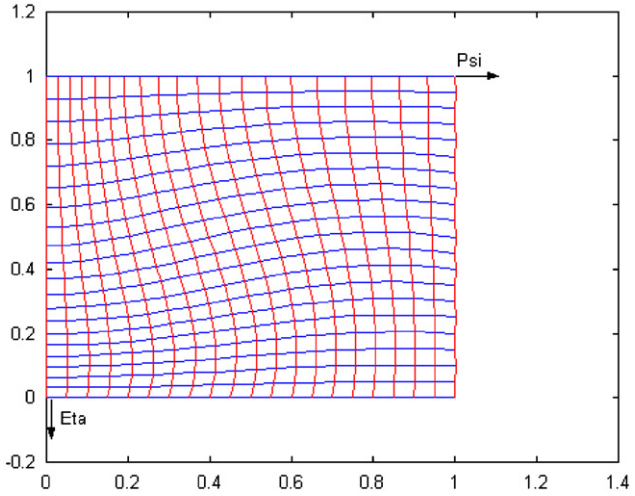

Fig. 9. First fully anti-symmetric mode for square plate: stiffness ratio = 1.0.

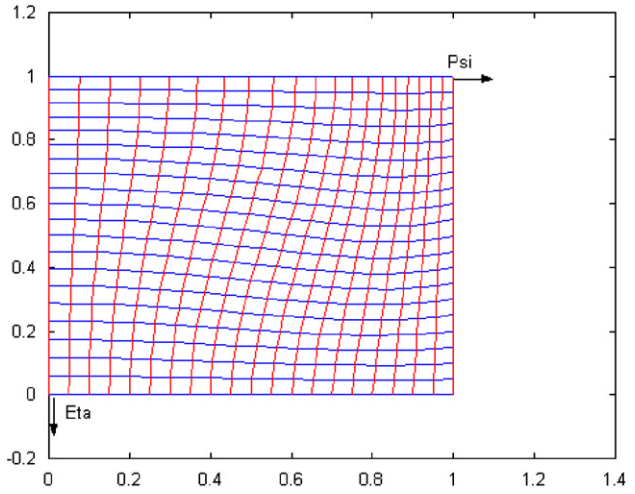

Fig. 10. First fully anti-symmetric mode for square plate: stiffness ratio = 2.0.

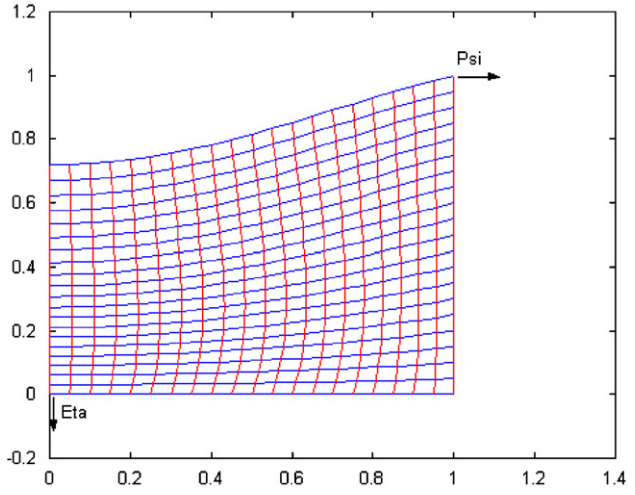

Fig. 11. First symmetric–anti-symmetric mode for square plate: stiffness ratio = 1.0.

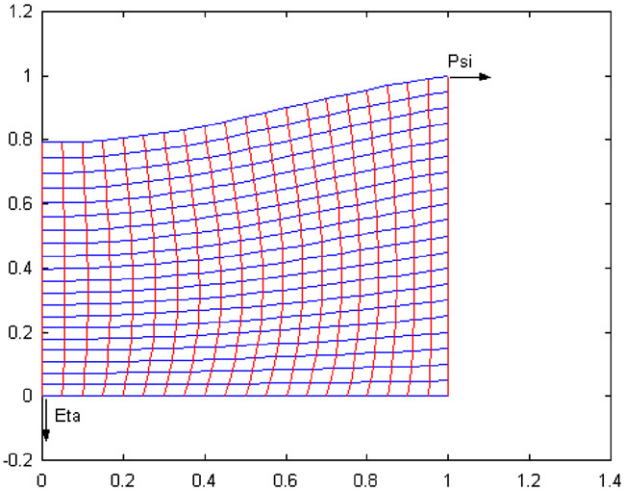

Fig. 12. First symmetric–anti-symmetric mode for square plate: stiffness ratio = 2.0.

4. Summary and conclusions

Accurate analytical type solutions have been obtained for the free in-plane vibration eigenvalues and mode shapes of rectangular orthotropic plates. The work is essentially a continuation of earlier work related to isotropic plates.

The dimensionless differential equations governing the in-plane vibratory behavior of orthotropic plates are formulated and the superposition method is again employed. Computed eigenvalues are tabulated for fully clamped plates over a range of plate aspect ratios and ratios of Youngs moduli. This appears to be the first analytical study of this practical engineering problem. Tabulated results provide other researchers with reference values against which their findings may be compared.

References

[1] N.S. Bardell, R.S. Langley, J.M. Dunson, On the free in-plane vibration of isotropic rectangular plates, *Journal of Sound and Vibration* 191 (3) (1996) 459–467.

[2] D.J. Gorman, Free in-plane vibration analysis of rectangular plates by the method of superposition, *Journal of Sound and Vibration* 272 (2004) 831–851.

[3] D.J. Gorman, Accurate analytical type solutions for the free in-plane vibration of clamped and simply supported rectangular plates, *Journal of Sound and Vibration* 276 (2004) 311–333.

[4] D.J. Gorman, Free in-plane vibration analysis of rectangular plates with elastic support normal to the boundaries, *Journal of Sound and Vibration* 285 (2005) 941–966.

[5] J. Du, W.L. Li, G. Jin, T. Yang, Z. Liu, An analytical method for the in-plane vibration analysis of rectangular plates with elastically restrained edges, *Journal of Sound and Vibration* 306 (2007) 908–927.

[6] D.J. Gorman, *Vibration Analysis of Plates by the Method of Superposition*, World Scientific Publishing Company, Singapore, 1999.

[7] R. Szillard, *Theory and Analysis of Plates*, Prentice-Hall, Englewood Cliffs, NJ, 1974.